Novel Carbon Nanotube-Based Nanostructures for High-Temperature Gas Sensing

Final Technical Report

Performance period: 09/01/2004-08/31/2008

Zhi Chen[1] and Kozo Saito[2]

Date of Report: Jan. 6, 2009

Grant Number: DE-FG26-04NT42171

[1]Department of Electrical & Computer Engineering

[2]Department of Mechanical Engineering

University of Kentucky

Lexington, KY 40506

[1]Phone: (859)257-2300 ext 268, Fax: (859)257-3092, E-mail: zhichen@engr.uky.edu

[2]Phone: (859) 257-6336, ext. 80639, Fax: (859) 257-3304, E-mail: saito@engr.uky.edu

DISCLAIMER

ABSTRACT

The primary objective of this research is to examine the feasibility of using vertically aligned multi-wall carbon nanotubes (MWCNTs) as a high temperature sensor material for fossil energy systems where reducing atmospheres are present. In the initial period of research, we fabricated capacitive sensors for hydrogen sensing using vertically aligned MWCNTs. We found that CNT itself is not sensitive to hydrogen. Moreover, with the help of Pd electrodes, hydrogen sensors based on CNTs are very sensitive and fast responsive. However, the Pd-based sensors can not withstand high temperature ($T<200°C$). In the last year, we successfully fabricated a hydrogen sensor based on an ultra-thin nanoporous titanium oxide (TiO_2) film supported by an AAO substrate, which can operate at 500°C with hydrogen concentrations in a range from 50 to 500 ppm.

TABLE OF CONTENTS

EXECUTIVE SUMMARY

The primary objective of this research is to examine the feasibility of using vertically aligned multi-wall carbon nanotubes (MWCNTs) as a high temperature sensor material for fossil energy systems where reducing atmospheres are present. The research will be pursued in three main areas: 1) study the growth mechanisms of MWCNTs using the flame synthesis technique and modification of the nanotemplate to improve the quality of the nanotubes for use in a gas sensing platform, 2) transform the modified vertically aligned CNTs into a capacitive type hydrogen sensor prototype to assess feasibility for high temperature applications, and 3) pursue theoretical modeling and numerical simulation of nanostructures, hydrogen gas sensors, and the flame synthesis for large-area nanotube growth.

In the initial period of research, we fabricated capacitive sensors for hydrogen sensing using vertically aligned MWCNTs. After extensive experiments, we found that AAO-based carbon nanotube sensors exhibit limited hydrogen sensitivity. In order to improve the sensitivity of the MWCNT based hydrogen sensors, we attempted using palladium (Pd) as electrodes because Pd is very sensitive to hydrogen. Using anodic aluminum oxides (AAOs) as substrates, the nanoporous Pd films were shaped by the AAOs' nanostructures. The nanoporous Pd films exhibit enhanced hydrogen-sensing properties, including enhanced response speed and sensitivity. We also found that CNT itself is not sensitive to hydrogen. Moreover, with the help of Pd electrodes, hydrogen sensors based on CNTs were built, which are very sensitive and fast responsive. However, the Pd-based sensors can not withstand high temperature ($T<200°C$). We examined the nanoporous platinum (Pt) film hydrogen sensors. Although Pt electrode can withstand high temperature, its capability for hydrogen absorption decreases as temperature increases. It is not feasible to use Pt for hydrogen sensing at high temperature.

In the last year, we successfully fabricated a hydrogen sensor based on an ultra-thin nanoporous titanium oxide (TiO_2) film supported by an AAO substrate, which can operate at 500°C. The TiO_2 film (~10nm) was prepared through electron-beam evaporation of titanium metal on a substrate followed by sintering at 600°C in a flowing synthetic air. The phase of the TiO_2 is completely rutile. This sensor is very robust and durable because of the TiO_2 film was formed on a silicon substrate with AAO. It was found that the sensitivity was significantly enhanced by the increased specific surface area of the TiO_2 thin film due to the porous AAO substrate. This sensor can operate at 500°C with hydrogen concentrations in a range from 50 to 500 ppm.

In our early work, we fabricated capacitive sensors for hydrogen sensing using vertically aligned MWCNTs. After extensive experiments, we found that AAO-based carbon nanotube sensors exhibit very low hydrogen sensitivity. In order to improve the hydrogen sensitivity, we used nanoporous palladium (Pd) films as electrodes because Pd is very sensitive to hydrogen. We also compared the sensors using Pd electrodes with those using Au electrodes to understand the intrinsic hydrogen sensing properties of CNTs.

1. Carbon Nanotube-Based Hydrogen Sensors

1.1 Fabrication of carbon nanotube-based hydrogen sensors

In this project, based on the AAO templates, hydrogen sensors has been fabricated and characterized. Fig. 1 shows two types of resistive hydrogen sensors: metal-electrode CNT sensor and CNT-supported Pd film sensor. A titanium layer (100 nm in thickness) and aluminum film (2.5 μm in thickness) were deposited, in turn, onto highly doped n-type Si wafers by e-beam evaporation. The Al film was anodized in a 0.3 M

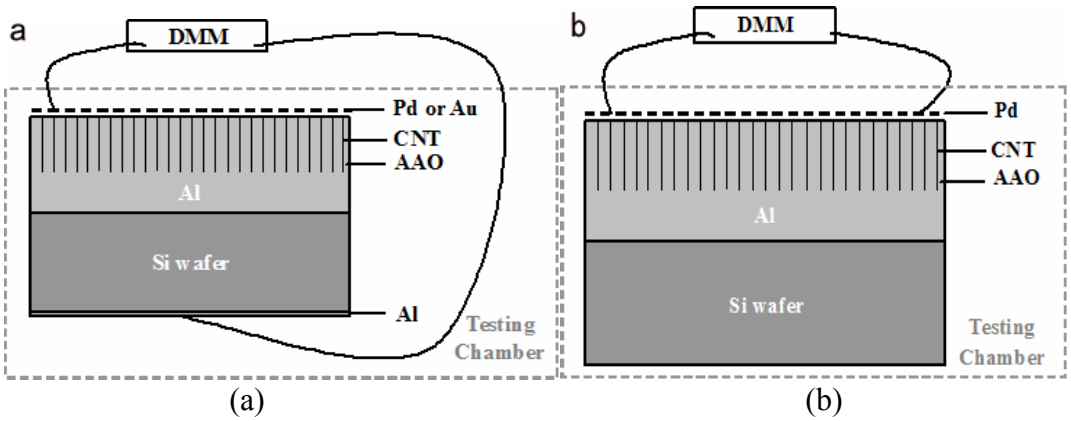

(a) (b)

Fig. 1 Structures of resistive hydrogen sensors: (a) metal-electrode CNT sensor and (b) CNT-supported Pd film sensor.

oxalic acid through a two-step method, and pore-widened in a 5wt% H_3PO_4 solution to obtain AAO template with pore diameters around 60-70 nm and pore lengths about 1 μm. Co catalysts were electrodeposited at the bottom of the AAO template. Aligned CNTs with partially crystallized (near amorphous) structures were grown in the AAO template through pyrolysis of 10% acetylene in Argon at 650°C. Detailed anodization, CVD processes and structural characterization of the aligned CNTs can be found elsewhere [1–3]. The samples were cut into small pieces.

Some as-cut samples were deposited with a bottom electrode of Al film (100 nm in thickness) through thermal evaporation, and a N_2 annealing at 450°C was conducted later to obtain an ohmic contact at the Si-Al interface. Pd electrode with a thickness of 45 nm was deposited, via r. f. sputtering, onto the upper surface. A Pd-electrode CNT sensor (Fig. 1a) was then fabricated through wire connections with the top Pd electrode and the bottom Al electrode. An Au-electrode CNT sensor (Fig. 1a) was fabricated by thermal-evaporating Au electrode (with a thickness of 45 nm) onto the upper surface of the CNTs. As hydrogen sensing characteristics of the top electrode of Pd are very useful for us to understand the roles of the electrode and CNTs in the metal-electrode CNT sensors, we also fabricated a CNT-supported Pd film sensor based on the top electrode (Fig. 1b) by using almost the same device structure.

1.2 Characterization of CNT-based hydrogen sensors

Fig. 2a shows the steady-state response of the sensors at various concentrations. It can be found that the Au-electrode CNT sensor shows no response to various concentrations of hydrogen gas at room temperature. But the Pd-electrode CNT sensor can detect medium concentration hydrogen (from 0.1% to 1.5% H_2). Typical response time of the Pd-electrode CNT sensor is about 3-4 minutes (Fig. 2b). And a reversible recovery can be obtained at H_2 concentrations below 1.5%. The CNT-supported Pd film sensor

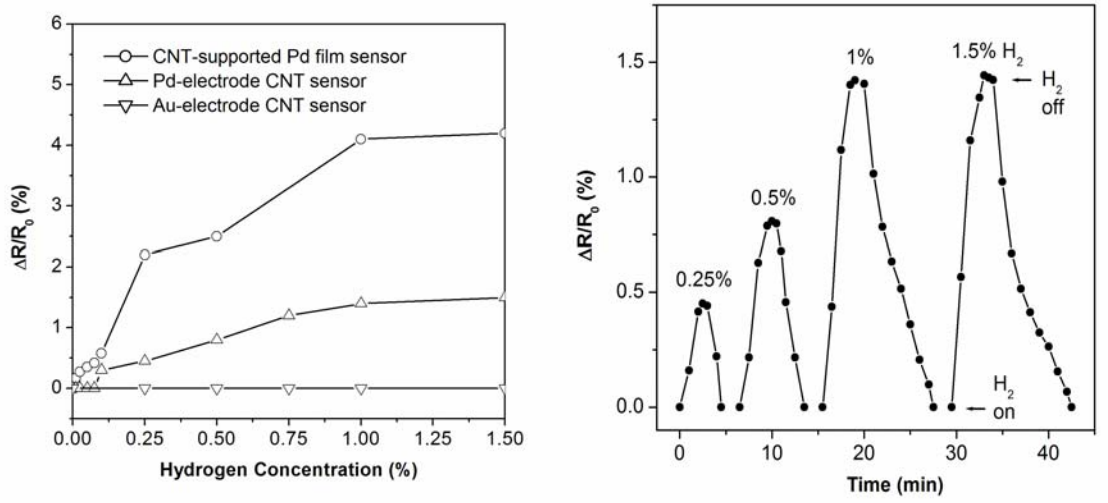

(a) (b)

Fig. 2 (a) Steady-state response of the metal- electrode CNT and the CNT-supported sensors at various H_2 concentrations. (b) Response of the Pd-electrode CNT sensor at medium H_2 concentrations. The measurements were carried out at a room temperature (~23°C).

is sensitive to hydrogen gas at both dilute and medium concentrations ranging from 100 ppm to 1.5% H_2 (Fig. 2b and Fig. 3). Typical response time of the CNT-supported Pd film sensor is less than 7 minutes for dilute H_2 gas (Fig. 2b), and less than 4 minutes for medium concentration hydrogen (Fig. 3). A reversible recovery can occur up to a high H_2 concentration of 1.5%. Above 1.5% H_2 the steady-state response value will decrease and the recovery is very slow, which suggests film instability due to excess volume expansion or stressing induced by absorption of H in the nanoporous Pd film. Thus, best performance range for the above CNT-supported Pd film sensor should be ranging from 100 ppm to 1.5% H_2.

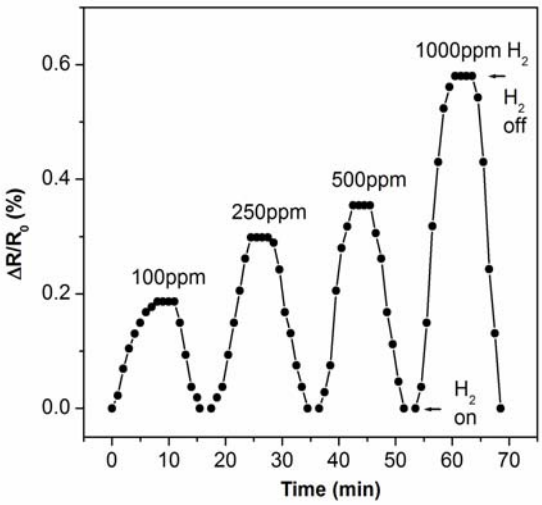

Fig. 3 Response of the CNT-supported Pd film sensor at dilute H_2 concentrations at ~23°C.

As can be found in many literatures, a dense Pd film can only detect medium concentration hydrogen (> 0.1% H_2) by showing a slow response or recovery. Obviously, with regard to detection limit, the nanoporous Pd film sensor supported by CNTs shows its advantage over traditional dense Pd film sensors due to a nanostructure-enhanced hydrogen sensing. Moreover, by comparison with

the narrower sensing range (250 ppm – 1% H_2) of nanoporous Pd film directly deposited onto AAO substrate [4-6], a wider detection range found with the CNT-supported Pd film here suggests that the CNTs in AAO template should be a good supporting material for providing better sensing stability than that from the AAO substrate.

As mentioned above, using Au-electrode for a CNT sensor does not work for resistive hydrogen sensing. And the Pd-electrode can make a CNT sensor be sensitive to hydrogen gas. Obviously, the only difference between the above two kinds of sensors is the type of the top metal electrode and it is well known that Au is not a hydrogen-sensitive material but Pd is. It can be confirmed that without the hydrogen-trapping material of Pd as a top electrode, the aligned CNTs grown in AAO template lack a capability for direct hydrogen sensing.

2. Pyrolytic Carbon-Stabilized Nanoporous Palladium Hydrogen Sensors

2.1 Fabrication of pyrolytic carbon-stabilized nanoporous palladium hydrogen sensors

We believe that better adhesion of a Pd film to the substrate is critical to improve its sensing capability in high concentration. Pyrolytic carbon was used to improve the adhesion between Pd and AAO [7]. With titanium film (100 nm in thickness) as a prime layer, aluminum film (2.5 μm in thickness) was deposited onto highly doped n-type Si wafers by e-beam evaporation. The Al film was anodized in 0.3M oxalic acid, through a two-step method and pore-widening in 5wt% H_3PO_4 solution to obtain anodic aluminum oxide (AAO) templates with pore diameters around 60-70 nm and pore lengths about 2 μm. A thin film of amorphous carbon (with a thickness of about several nanometers) [8] was deposited onto the AAO template through CVD pyrolysis of 10% acetylene at 650°C for 10 minutes. Detailed anodization and CVD processes can be found elsewhere [8,1,2]. Pd film with a nominal thickness of 45 nm was then deposited, via sputtering, onto the upper surface of the samples. For comparison, nanoporous Pd film sensors directly supported by AAO template and dense Pd film sensor directly supported by thermally oxidized n-type Si wafer were also prepared. Resistive sensor based on the Pd film was then fabricated and tested under various concentrations of H_2 in nitrogen (Fig. 4).

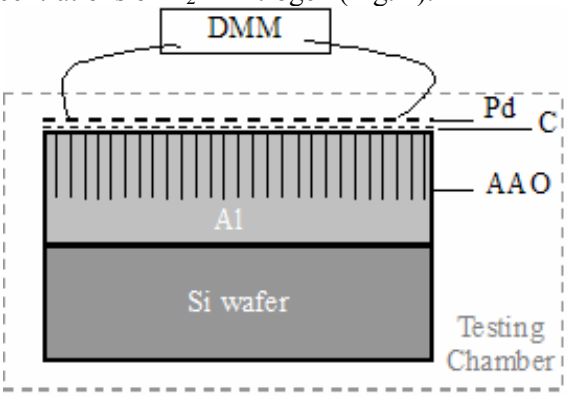

Fig. 4 Resistive hydrogen sensors based on pyrolytic C-supported nanoporous Pd film.

2.2 Characterization of pyrolytic carbon-stabilized nanoporous palladium hydrogen sensors

The steady-state response (relative resistance change, $\Delta R/R_0$) increases with increase of hydrogen concentrations (Figs. 5 and 6). At lower H_2 concentrations (less than 1000 ppm), the steady-state response value of the nanoporous carbon-supported Pd film sensor was found to be 0.4% at 250 ppm H_2 and up to 1.0% at 1000 ppm H_2. At higher H_2 concentrations (less than 10%), a steady-state response value up to 15.6% at 10% H_2 can be found in the nanoporous carbon-supported Pd film sensor. On the other hand, a dense Pd film sensor directly supported by thermally oxidized Si wafer can only detect medium-

concentration hydrogen (below 1%H_2). And a nanoporous Pd film sensor directly supported by the AAO template could have a little wider detection range (from medium-concentration hydrogen down to dilute hydrogen). This suggests that the film damage due to excess volume expansion or stressing induced by absorption of H in the nanoporous Pd film have not occurred for hydrogen concentrations as high as 10%. On the contrary, at hydrogen concentrations above 1%, the steady-state response of the dense Pd film and the nanoporous Pd film directly supported by AAO template began to decrease due to expansion-induced damage, which hindered a detection of high-concentration hydrogen. Thus, with regard to detection limit, the carbon-supported nanoporous Pd film sensor shows its great advantage of wide-range (250 ppm – 10% H_2) sensing over traditional dense Pd film sensors, AAO-supported Pd film sensor and even the break-junction Pd nanowires.

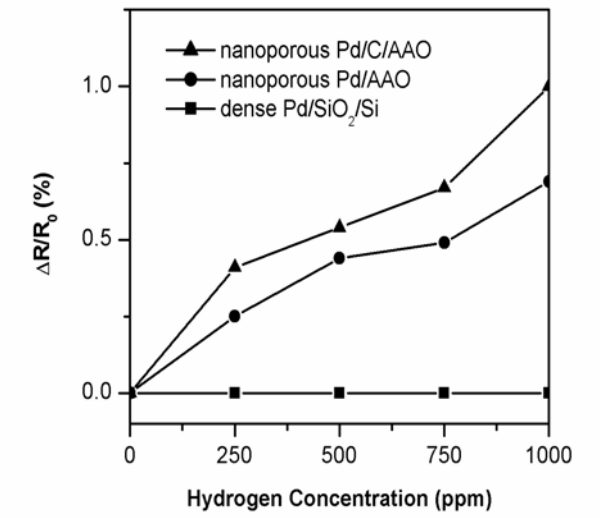

Fig. 5 Steady-state response of the nanoporous carbon-supported sensor at dilute H_2 concentrations at ~23°C. Response curves of an AAO-supported sensor and a dense film sensor supported by oxidized wafer are also presented.

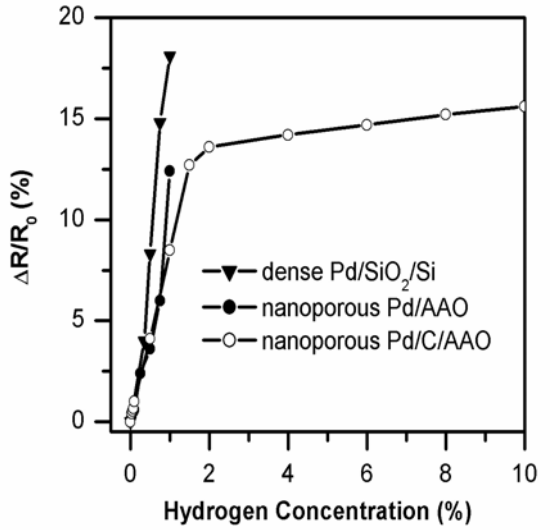

Fig. 6 Steady-state response of the nanoporous carbon-supported sensor at various H_2 concentrations ~23°C. Response curves of an AAO-supported sensor and dense film sensor supported by oxidized wafer are also presented.

As shown in Figs. 7 and 8a, typical response time (the time for reaching 90% variation of the film resistance after introduction of hydrogen gas) of the carbon-supported nanoporous Pd film sensor is less than 4 minutes for dilute H_2 gas. At H_2 concentrations of 2%, the response time becomes 90s, and it only takes less than 30 seconds to have an 8% variation of film resistance. With increase of the H_2 concentration to 10%, the response time is less than 30s. It should be mentioned that, in the balancing atmosphere of nitrogen, there was always a slight drift down of the film resistance for our nanoporous Pd film sensors. Such a drift down of the film resistance (after a full recovery of the starting resistance) could be found in Fig. 8b, which shows nearly reproducible response of the pyrolytic carbon-supported Pd film sensor under repeated sensing testing with 1% H_2 in nitrogen. The drift down of film resistance in the inert atmosphere was so small that it could not affect a normal sensing performance.

The wide-range sensing ability of the nanoporous carbon-supported hydrogen sensor here should be mainly attributed to the nanoporous structures of the Pd film. As the specific area of the nanoporous Pd film is much larger than that of a dense Pd film, hydrogen gas tends to dissociate easily on the surface of the nanoporous Pd film. The nanoscale thickness (45nm) and patterned morphology aids the diffusion of H_2 into the Pd lattice. Thus, during a hydrogen sensing process, rapid absorption and desorption of

hydrogen can occur accompanying with noticeable resistance variation, which results in enhanced hydrogen sensing for dilute hydrogen gas as low as 250 ppm.

It has been established that lattice or volume expansion of dense Pd film upon absorption of high-concentration hydrogen can cause considerable stressing in the dense Pd film or stress mismatch at the film/substrate interface, which finally leads to the blistering of dense Pd film and thus the sensor loses sensing stability (i.e., reversibility and durability, etc.) [9]. The stressing problem also exists in our previous nanoporous Pd film sensors [5]. Therefore, any effort to alleviate such a stressing will help to stabilize the Pd deposition and thus to obtain an improved H sensing performance (higher upper detection limit). By comparison with the AAO-supported Pd films that can only detect up to 1% H_2, the nanoporous Pd film supported by the C-coated AAO template can detect high-concentration hydrogen without a failure. This suggests that the pyrolyzed carbon layer help to minimize the strain between Pd and the aluminum oxide substrate and thus remarkably enhance the film stability upon absorption of high-concentration hydrogen.

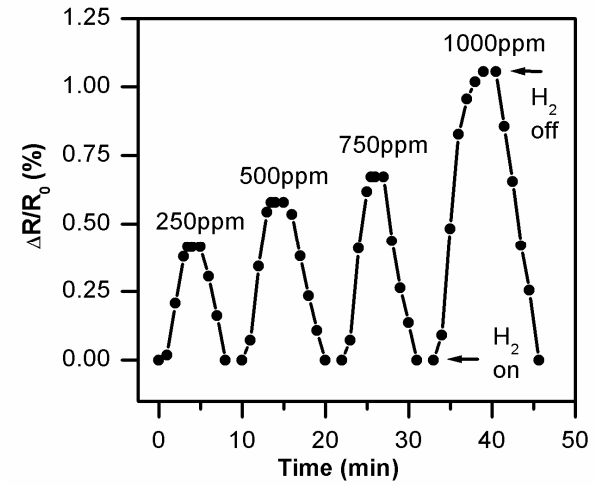

Fig. 7 Response of the nanoporous carbon-supported Pd sensor at dilute H_2 concentrations ~23°C.

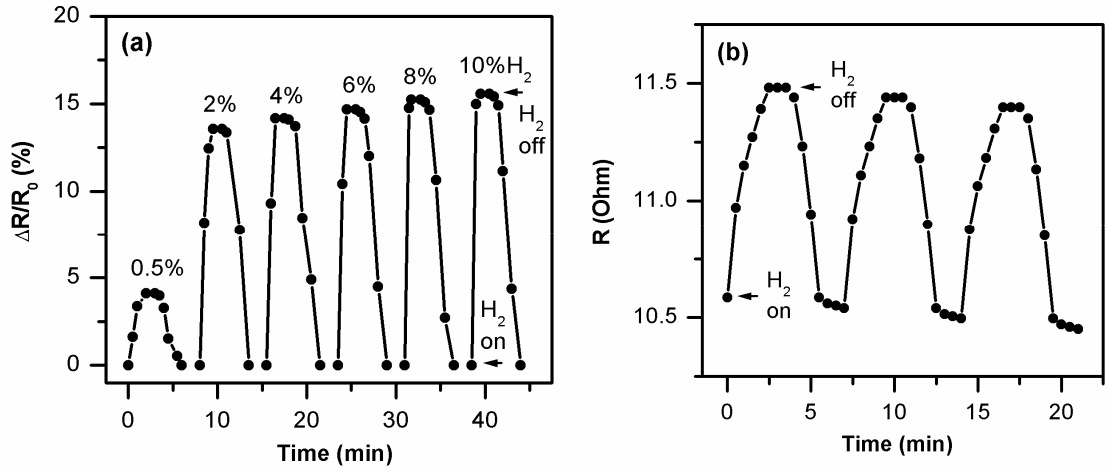

Fig. 8 (a) Response of the nanoporous carbon-supported Pd sensor at higher H_2 concentrations ~23°C, and (b) typical variation of the resistance under repeated testing between nitrogen and 1% H_2 balanced with nitrogen ~23°C.

3. Nanoporous TiO_2 thin film hydrogen sensors operating at 500°C

In the past few years, hydrogen sensors based on the n-type titanium oxide (TiO_2) films with the thickness of microns or sub-microns have been studied extensively [10-13]. Among these reported devices, films composed of self-organized TiO_2 nanotube arrays [12,13] are proved to have much higher sensitivities over bulk films. The sensing principle is always based on the significant and abrupt change in resistance. Most of such nano-porous devices are fabricated on Ti metal plate or foil, and the top TiO_2 is prepared by anodization followed by sintering at elevated temperatures. The major component of the TiO_2 film obtained by this method is anatase, a meta-stable phase of TiO_2, which gradually converts into rutile, the preferred polymorph of TiO_2, at above 430°C for nanotubes [14] or 465°C for nano-crystalline [15]. This causes instability of the sensors. Due to this reason, most of the TiO_2 nanotube sensors were characterized at below 400°C [12,13]. Furthermore, the metal substrate (Ti foil) is not a durable material due to its high chemical activity at elevated temperatures.

Although it had been found that porous films with rutile as the major phase are sensitive to hydrogen [16], the sensitivity was quite low [17] or even null [18], especially at above 400°C [16-18]. Jun et. al. [19] reported rutile-phased sensors prepared by thermal oxidation, with high sensitivity and swift response. However, the substrate was still a titanium metal plate, which can be further oxidized or electrically shorted. The operating temperature was also limited to less than 300°C. Therefore, the advantage of the rutile-phased sensor (thermal stability) was not demonstrated. In this report, we will present fabrication and characterization of hydrogen sensors based on ultra-thin rutile-phased TiO_2 films supported AAO, which can operate at 500°C.

3.1 Sensor fabrication

Three substrates were prepared: porous anodized aluminum oxide, α-phased alumina plate, 300nm-thick thermal silicon oxide on top of a (100) silicon wafer. The AAO was prepared in our lab while the later two substrates were commercially available. In this paper, the device based on porous anodized aluminum oxide will be referred to as "PA" (porous AAO), that based on α-phased alumina as "CP" (ceramic plate), and that based on silicon oxide on a silicon wafer as "WA" (wafer).

The preparation of AAO started from a commercial (100) silicon wafer with a 300nm-thick thermal silicon oxide on the surface, which was covered with a 2.2μm aluminum metal layer through e-beam evaporation. A two-step anodization procedure was used, in which anodization was performed on an Al metal layer in a 0.3M oxalic aqueous solution under a bias voltage of 40V, with a platinum plate served as the cathode. Until the Al metal layer was completely converted into porous Al_2O_3, the sample was rinsed by de-ionized water and then immersed in a 0.6M phosphoric acid solution for 10 min. for pore widening.

After rinsing in de-ionized water again and drying, the AAO sample ("PA"), along with the commercial α-alumina ("CP") and the (100) silicon wafer with 300 nm thermal oxide ("WA"), were all coated with an approximate 9 nm titanium metal layer through e-beam evaporation. According to some previous research [20,21], this thin Ti layer would be oxidized completely when the evaporator chamber was vented to atmosphere. Nonetheless, since the samples were expected to work at 500°C, the samples were sintered at 600ºC for 6 h in synthetic air with a flow rate of 1000 ml/min. After sintering, the TiO_2 film thickness on the WA sample was found to be 10 nm by ellipsometry measurement and the crystal phase of the thin layer was examined by a Siemens D500 X-ray diffactometer (XRD). However, 10 nm is too thin to produce any significant diffraction in the XRD spectrum. Therefore, a TiO_2 film of about 100 nm was prepared exactly following the steps described above (evaporation of Ti metal and sintering in synthetic air at 600ºC for 6h). The crystal phase was determined on this thicker film. A Hitachi S-9300 scanning electron microscope (SEM) was used to study the surface morphology of the samples.

Platinum was used as cathode in anodization, due to its chemical inertia. For the hydrogen sensors, two Pt electrodes arranged in an interdigit configuration were fabricated on the 10 nm-thick TiO_2 film for all the three samples. The spacing between digits of the two electrodes is 5 μm, as shown in Fig. 1. All the three samples were equipped with the same number of digits by photolithography. However, the Pt layer on the WA sample peeled off entirely during the lift-off of the photoresist due to the extreme smoothness of the front side (polished) of the silicon wafer. To solve this problem, TiO_2 thin film and Pt electrodes were fabricated on the backside (non-polished) of the silicon wafer. Even though, the electrodes and digits of the WA sample still experienced severe damage through the lift-off, and the signal magnitude of the device was unavoidably attenuated. The entire procedure for fabricating the PA sample is illustrated in Fig. 9. For CP and WA, the preparation procedures were quite similar to but simpler than that for PA.

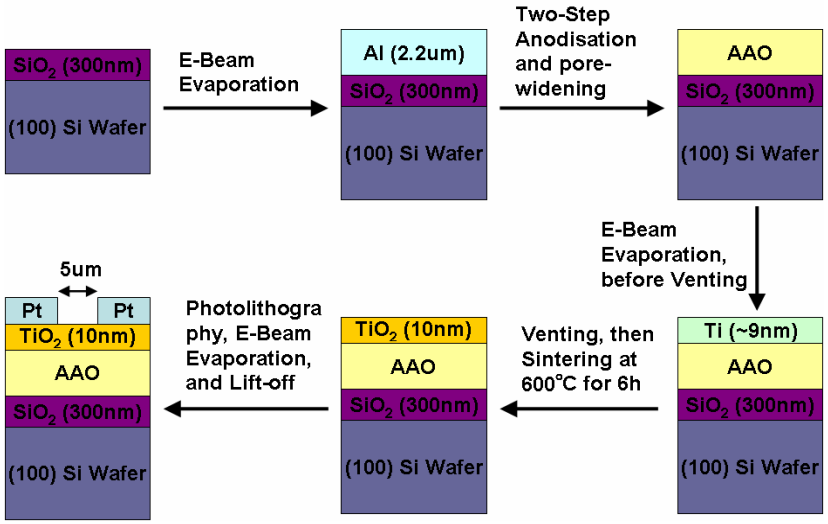

Fig. 9 Fabrication steps for preparation of porous AAO, an ultra-thin TiO_2 film, and Pt electrodes.

Resistance measurements at different H_2 concentration levels (5 ppm-500 ppm) were performed using an MASTECH M3900 multimeter at 500ºC. Nitrogen was used as the background gas. The recorded resistance values were then inverted to conductance. Since the conductance of 10 nm TiO_2 is close to zero in the pure nitrogen ambient, absolute conductance values will be used to define the sensor responses in this presentation.

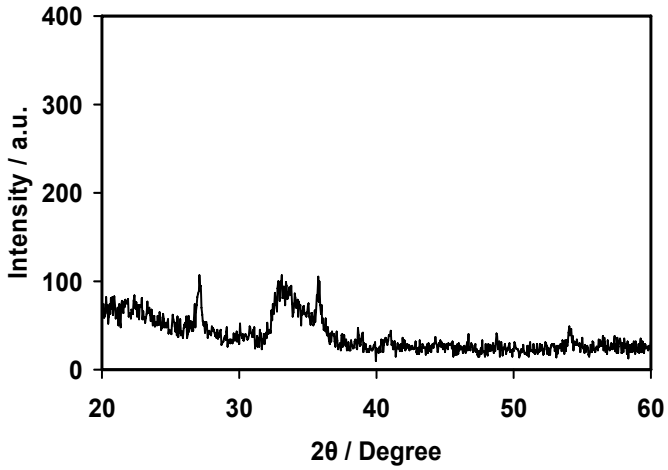

Fig. 10 a XRD spectrum of a 100 nm TiO_2 film that was produced from a 90 nm Ti metal layer on AAO/SiO_2/Si substrate through sintering at 600°C for 6 h in synthetic air with a flow rate of 1000 ml/min.

3.2 Results and discussion

Fig. 10 shows the XRD spectrum for the 100 nm-thick TiO_2 prepared by oxidizing an approximate 90 nm-thick Ti metal film at 600ºC for 6 h in synthetic air with a flow rate of 1000 ml/min. The substrate is the same as that of the PA sample (?). There are three significant peaks at around 27°, 33°, and 36°, as well as two less significant peaks at about 41° and 54°. Considering the wavelength of the incident X-ray is 1.54Å (Cu-Kα), we can figure out through Bragg's Law by referring to the lattice constants of all possible crystals on the surface [22]. All the peaks, but the wide one at 33° that represents the silicon (200) plane, are corresponding to the lattice constants of rutile. Therefore, the metallic Ti was completely transformed into

TiO_2 and rutile was the only phase that was observed in the 100 nm TiO_2 film. Since the 10 nm TiO_2 thin layers on PA, CP, and WA were sintered at the same condition as that of the 100 nm film in Fig. 3, it is reasonable to draw a conclusion that rutile is the only crystal phase in all the 10 nm-thick TiO_2 films as well.

The surface morphology of the TiO_2 films on substrates PA, CP, and WA were shown in Fig. 11. For the WA sample (See Fig. 11 (c)), although it was the backside of a commercial silicon wafer, the surface was so flat that almost no significant features can be observed. All the three samples were covered with a 10 nm TiO_2 film. However, since this film was ultra thin, the coated surfaces look very similar to the original substrates in the SEM, because the gold coating for SEM that was sputtered on the specimen surface to make them conductive is already around 20 nm.

Response transients of the PA sample to 5ppm-500ppm H_2 at 500°C are shown in Fig. 12. The baseline conductance, at which no hydrogen was introduced but only pure nitrogen was in the ambient, was found to be ~1.4 μS (~0.7 MΩ). This means that the conductance change due to the introduction of 5ppm-500ppm hydrogen is about 30~120 time. For example, at a hydrogen concentration level of 50 ppm, the stabilized conductance is ~0.1 mS, thus the change from the baseline is around 70 times. Although it is less than that of some reported anatase-phased TiO_2 sensors with a resistance drop of 10^3~10^4 times upon introduction of 100 ppm H_2 [17], this sensitivity is large enough. More importantly, the data in Fig. 12 was obtained from a pure rutile-phased sample, supported by an insulating substrate which is more robust and durable. Upon introduction of hydrogen, the conductance increased rapidly. For all the H_2 concentration levels measured in Fig. 12, the time delay to reach 50% of the platform conductance ($t_{50\%}$) was always about 5~10s. The recovery was quicker than the response ($t_{50\%}$≤5s) for all concentration levels, indicating a quite fast removal of hydrogen from the device.

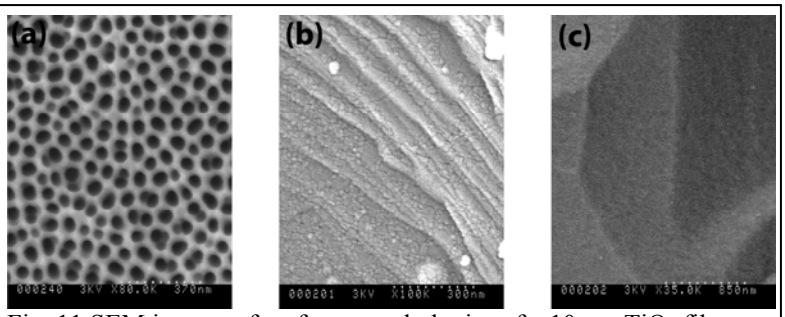

Fig. 11 SEM images of surface morphologies of a 10 nm TiO_2 film on PA (a), CP (b), and WA (c) substrates, after sintering of the Ti film at 600°C for 6 h in a flowing synthetic air.

The influence of specific surface area on H_2 sensitivity can be demonstrated by comparing Fig. 13a with Fig. 11. It is should be noted that the sensitivity increases with the increase in the surface porosity. The large surface area of the PA sample results in the largest response. In the PA sample, the conductance changes from close-to-zero (~1.4μS) to 0.05~0.18 ms, corresponding to an increment of ~30-120 times (see Fig. 12 for details). Whereas in the WA sample, the surface is so flat that little feature can be observed at the magnification of 35K times; this poor roughness causes weak sensitivity. Also, the peeling-off of the Pt electrode during the fabrication degraded the performance. This drawback suggests that TiO_2 directly on a thick SiO_2 thermally grown on a silicon wafer, is not good for hydrogen detection. The CP sample has a moderate surface roughness and the response is fairly significant although much less than that of the PA. In general, the larger the specific surface area, the more active sites or defects in which hydrogen adsorption occurs, and therefore more electrons are accumulated on the surface of the 10 nm-thick TiO_2.

Typical response transients of the CP and WA samples are shown in Fig. 7. The WA sample showed not only quite weak sensitivity (Fig. 13a), but also slow response. As summarized in Fig.13b, in response to 50 ppm H_2, the time delay to reach 50% of the platform conductance ($t_{50\%}$) of the WA sample is as long as 55s, which is several times of those of the PA (5s) and the CP (11s). However, the recovery time of the

WA is about 10s, which is not much longer than those of the PA (4s) and the CP (7s). This phenomenon, in which TiO_2 surfaces lack of porosity show slow response, has been noticed in previous studies [19]. A reasonable explanation is that the nano-scaled geometrical flaws on the TiO_2 surface produce an enhanced catalysis effect that accelerates the adsorption of H_2. According to the theory constructed for surface chemical reactions long time ago [23], the reaction rate is directly determined by the surface density of active sites, which increases with the specific surface area. Therefore, large specific surface area results in fast response. A moderate response rate (t_{50}=11s) was observed on the CP sample due to its moderate surface roughness (Fig. 11b).

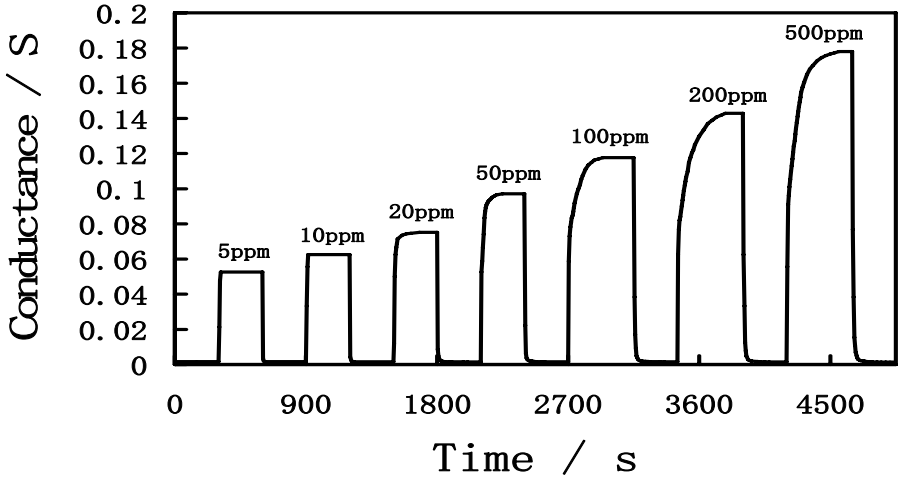

Fig. 12 Response transients of the PA sample to 5ppm, 10ppm, 20ppm, 50ppm, 100ppm, 200ppm, and 500ppm H_2 at 500°C.

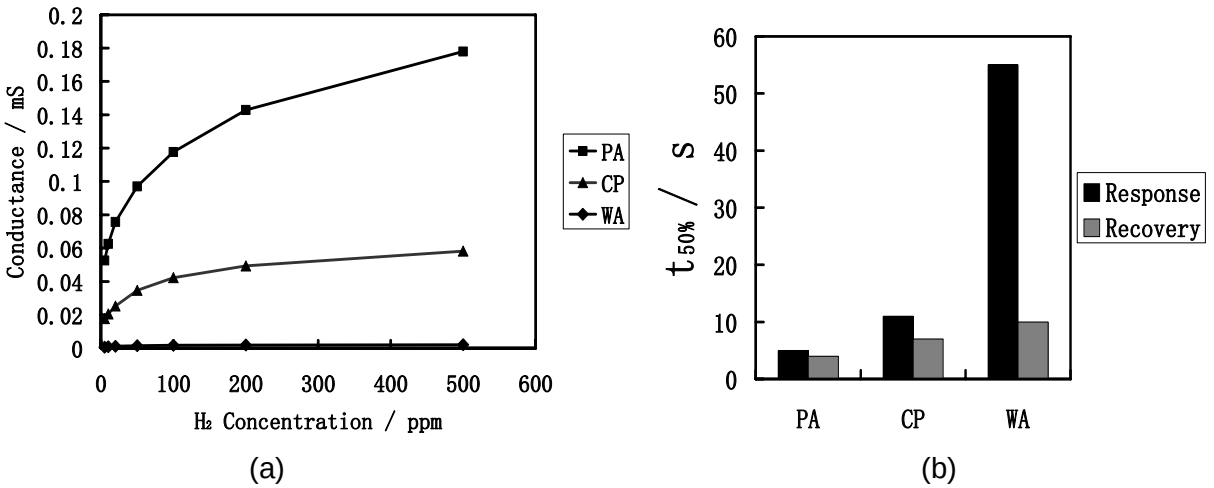

Fig. 13 (a) Conductance responses to 5ppm-500ppm hydrogen gas of PA, CP and WA, the operating temperature was 500°C for all the three samples. (b) Response/recovery times in terms of $t_{50\%}$ for the PA, CP and WA samples

The sensing mechanism of anatase-phased TiO_2 nanotube has been studied rather thoroughly [24, 25]. The large, fast, and reversible response is attributed to a "spill-over" mechanism, in which hydrogen molecules absorb onto the platinum electrodes, dissociating into atoms or even protons, and finally spill out of the Pt, diffusing into the surface layer of the TiO_2. Once the active H or H^+ chemically absords at the interstitial positions in the oxide lattice structure, partial electron charge is transferred to the n-type

TiO_2 and the conductance increases rapidly [26]. Also, the sensitivity is enhanced by the large relative surface [25].

It is reasonable to consider the sensing principle of the sensors presented in this paper as a spill-over mechanism as well, due to the considerable resistance drop and the swift response transients (Fig. 5). The swiftness of the transients indicates that the sensitivity is primarily from the chemisorption of H but not H^+, which, as a charged ion, causes severe hysteresis when chemically adsorbed. Since the background gas is pure nitrogen and the signal reaches full recovery, the "oxygen-removal" mechanism [27], involving desorption of the oxygen adsorbates on the oxide surface by combination with hydrogen to form water ($O_{ad}+2H_{ad}\rightarrow H_2O$), is definitely not applicable. Furthermore, the fast and reversible response has ruled out the possibility of hydrogen reduction of Ti^{4+} into Ti^{3+} [28].

However, the relative low sensitivity and instantaneous recoveries of all the three samples (Fig. 8) suggest that the spill-over mechanism is somewhat different from that of the anatase nanotubes. The crystal structure of rutile (a=4.59Å, c=2.96Å) is much more close-packed than that of anatase (a= 3.78Å, c= 9.51Å) [29]. As a result, the specific weight or density of rutile is 4.25, which is heavier than that of anatase, 3.88 [29]. Therefore, rutile accommodates less amount of impurity or adsorbate (e.g., atomic hydrogen) at the interstitial spaces inside the lattice than anatase does, and the corresponding H_2 sensitivity is expected to be lower than that of the later, even when the specific surface area of the rutile film is quite large (e. g., the PA sample). On the other hand, the incapability of rutile in holding hydrogen at interstitial lattice positions offers ultra-fast recovery – a characteristic that can be considered as an advantage over those anatase sensors.

4. Conclusions

We found that CNT itself is not sensitive to hydrogen. Moreover, with the help of Pd electrodes, hydrogen sensors based on CNTs are very sensitive and fast responsive. However, the Pd-based sensors can not withstand high temperature (T<200°C). We successfully fabricated a hydrogen sensor based on an ultra-thin nanoporous titanium oxide (TiO_2) film supported by an AAO substrate, which can operate at 500°C with hydrogen concentrations in a range from 50 to 500 ppm. The stable rutile phase obtained by annealing the TiO_2 film at 600°C makes it possible to fabricate durable high-temperature hydrogen sensors. The roughness of the AAO surface also helps the attachment of thin-film metal electrodes. Although rutile is a less-sensitive material to hydrogen, the response is greatly enhanced by the large porosity of AAO and ultra-fast recovery is obtained as an advantage over anatase.

References

1. J. Li, C. Papadopoulos, J.M. Xu, M. Moskovits, Highly-ordered carbon nanotube arrays for electronics applications, Appl. Phys. Lett. 75 (1999) 367–369.
2. W.C. Hu, D.W. Gong, Z. Chen, L.M. Yuan, K. Saito, P. Kichambare, C.A. Grimes, Growth of well-aligned carbon nanotube arrays on silicon substrate using porous alumina film as nano-template, Appl. Phys. Lett. 79 (2001) 3083–3085.
3. J. Li, M. Moskovits, T.L. Haslett, Nanoscale electroless metal deposition in aligned carbon nanotubes, Chem. Mater. 10 (1998) 1963–1967.
4. Dongyan Ding and **Zhi Chen**, "Volume-Expansion-Enhanced Pinning of Nanoporous Pd Films for Detection of High-Concentration Hydrogen," Sensor Letters, vol. 4, 331-333 (2006).
5. Dongyan Ding, **Zhi Chen**, and Chi Lu, "Hydrogen sensing of nanoporous palladium films supported by anodic aluminum oxides," Sensors & Actuators B, vol. 120, 182-186 (2006).
6. Dongyan Ding, **Zhi Chen,** Suresh Rajaputra and Vijay Singh, "Hydrogen sensors based on aligned carbon nanotubes in anodic aluminum oxide template with palladium as top electrodes," Sensors & Actuators B, vol. 124, 12-17 (2007).

7. Dongyan Ding and **Zhi Chen**, "Pyrolytic Carbon-Stabilized Nanoporous Palladium Film for Wide-Range Hydrogen Sensing," Adv. Mater., vol. 19, 1996–1999 (2007).
8. K. B. Shelimov, D. N. Davydov, M. Moskovits, *Appl. Phys. Lett.* **2000**, 77, 1722–4.
9. M. Armgarth, C. Nylander, *IEEE Electron Device Lett.* **1982**, EDL-3, 384.
10. L. D. Birkefeld, A. M. Azad, S. A. Akbar, Carbon Monoxide and Hydrogen Detection by Anatase Modification of Titanium Dioxide, J. Am. Ceram. Soc. 75 (1992), 2964-2968.
11. H. Tang, K. Prasad, R. Sanjines, F. Levy, TiO2 anatase thin films as gas sensors, Sens. Actuators B 26 (1995) 71-75.
12. M. Paulose, O. K Varghese, G. K. Mor, C. A. Grimes, K. G. Ong, Unprecedented ultra-high hydrogen gas sensitivity in undoped titania nanotubes, Nanotechnology 17 (2006) 398-402.
13. C. A. Grimes, Synthesis and application of highly ordered arrays of TiO2 nanotubes, J. Mater. Chem. 17 (2007) 1451-1457.
14. O. K. Varghese, D. Gong, M. Paulose, C. A. Grimes, E. C. Dickey, Crystallization and high-temperature structural stability of titanium oxide nanotube arrays, J. Mater. Res. 18 (2003) 156-165.
15. H. Zhang, J. F. Banfield, New kinetic model for the nanocrystalline anatase-to-rutile transformation revealing rate dependence on number of particles, Am. Mineral. 84 (1999) 528-535.
16. Y. Shimizu, N. Kuwano, T. Hyodo, M. Egashira, High H2 sensing performance of anodically oxidized TiO2 film contacted with Pd, Sens. Actuators B 83 (2002) 195-201.
17. H. Kim, W. Moon, Y. Jun, S. Hong, High H_2 sensing performance in hydrogen trititanate-derived TiO2, Sens. Actuators B 120 (2006) 63-68.
18. V. Guidi, M. C. Carotta, M. Ferroni, G. Martinelli, L. Paglialonga, E. Comini, G. Sberveglieri, Preparation of nanosized titania thick and thin films as gas-sensors, Sens. Actuators B 57 (1999) 197-200.
19. Y. Jun, H. Kim, J. Lee, S. Hong, High H2 sensing behavior of TiO2 films formed by thermal oxidation, Sens. Actuators B 107 (2005) 264-270.
20. Henrik Ekstroma, Bjorn Wickman, Marie Gustavsson, Per Hanarp, Lisa Eurenius, Eva Olsson, Goran Lindbergh, Nanometer-thick films of titanium oxide acting as electrolyte in the polymer electrolyte fuel cell, Electrochim. Acta 52 (2007) 4239-4245.
21. M. Gustavsson, H. Ekstromc, P. Hanarp, L. Eurenius, G. Lindbergh, E. Olsson, B. Kasemoa, Thin film Pt/TiO2 catalysts for the polymer electrolyte fuel cell, J. Power Sources 163 (2007) 671-678.
22. W. F. McClune (Ed.), Powder Diffraction File: Inorganic Phases, Alphabetical Index, JCPDS International Center for Diffraction Data, Swarthmore, PA, US, 1987
23. P. W. Atkins, Physical Chemistry, 7th Edition, W. H. Freeman, New York, NY, US, 2002.
24. O. K. Varghese, D. Gong, M. Paulose, K. G. Ong, C. A. Grimes, Hydrogen sensing using titania nanotubes, Sens. Actuators B 93 (2003) 338-344.
25. O. K. Varghese, D. Gong, M. Paulose, K. G. Ong, E. C. Dickey, C. A. Grimes, Extreme changes in the electrical resistance of titania nanotubes with hydrogen exposure, Adv. Mater. 15 (2003) 624-627.
26. U. Roland, R. Salzer, T. Braunschweig, F. Roessner, H. Winkler, Investigations on hydrogen spillover: Part 1 - Electrical conductivity studies on titanium dioxide, J. Chem. Soc., Faraday Trans. 91 (1995) 1091-1095.
27. G. C. Mather, F. M. B. Marques, J. R. Frade, Detection Mechanism of TiO2-based Ceramic H2 Sensors, J. Eur. Ceram. Soc. 19 (1999) 887-891.
28. R. M. Walton, D. J. Dwyerc, J. W. Schwank, J. L. Glan, Gas sensing based on surface oxidation/reduction of platinum-titania thin films I. Sensing film activation and characterization, Appl. Surf. Sci. 125 (1998) 187-198.
29. D. R. Lide (Ed.), CRC Handbook of Chemistry and Physics, Internet Version 2005, <http://www.hbcpnetbase.com>, CRC Press, Boca Raton, FL, US, 2005.

List of Publications Supported by this Grant

Journal publications

1. Z. Chen and C. Lu, "Humidity sensors: a review of materials and mechanisms," Sensor Letters vol. 3, pp. 274-295 (2005). (Invited)
2. Z. Chen and H. Zhang, "Mechanisms for formation of a one-dimensional array of nanopores by anodic oxidation," J. Electrochem. Soc. vol. 152, no. 12, pp. D227-D231 (2005).
3. H. Zhang, Z. Chen, T. Li, and K. Saito, "Fabrication of a one-dimensional array of nanopores on a silicon substrate," J. Nanosci. & Nanotechnol. vol. 5, pp. 1745-1748, 2005.
4. Dongyan Ding and Zhi Chen, "Volume-Expansion-Enhanced Pinning of Nanoporous Pd Films for Detection of High-Concentration Hydrogen," Sensor Letters, vol. 4, 331-333 (2006).
5. Dongyan Ding, Zhi Chen, and Chi Lu, "Hydrogen sensing of nanoporous palladium films supported by anodic aluminum oxides," Sensors & Actuators B, vol. 120, 182-186 (2006).
6. Dongyan Ding and Zhi Chen, "Pyrolytic Carbon-Stabilized Nanoporous Palladium Film for Wide-Range Hydrogen Sensing," Adv. Mater., vol. 19, 1996–1999 (2007).
7. Dongyan Ding, Zhi Chen, Suresh Rajaputra and Vijay Singh, "Hydrogen sensors based on aligned carbon nanotubes in anodic aluminum oxide template with palladium as top electrodes," Sensors & Actuators B, vol. 124, 12-17 (2007).
8. T.X. Li, H.G. Zhang, F.J. Wang, Z. Chen, and K. Saito, "Synthesis of carbon nanotubes on Ni-alloy and Si-substrates using counterflow methane–air diffusion flames," Proceedings of the Combustion Institute, vol. 31, 1849-1856 (2007).
9. Hongguo Zhang and Zhi Chen, "A Horizontally Aligned One-Dimensional Carbon Nanotube Array on a Si Substrate," J. Electrochem. Soc., vol. 154, H124-H126 (2007).
10. Chi Lu, Zhi Chen, and Kozo Saito, "Hydrogen sensors based on Ni/SiO_2/Si MOS capacitor," Sensors & Actuators B, vol. 122, 556-229 (2007).
11. T. X. Li, K. Kuwana, K. Saito, H. Zhang, Z. Chen, "Temperature and carbon source effects on methane–air flame synthesis of CNTs," Proceedings of the Combustion Institute, vol. 32, 1855–1861 (2009).
12. Chi Lu and Zhi Chen, "High-Temperature Resistive Hydrogen Sensor Based on Ultra-Thin Nanoporous TiO_2 Film on Anodic Aluminum Oxide," Sensors & Actuators B, submitted (2008).

Conference Proceedings and Presentations

1. Z. Chen and K. Saito, "Novel Carbon Nanotube-Based Nanostructures for High-Temperature Gas Sensing," Abstract for US Department of Energy UCR program PI Meetings, Pittsburgh, PA, 06/06-06/08/2005
2. Dongyan Ding and Zhi Chen, "Nanoporous Pd Film Sensors for Detection of High Concentration Hydrogen," the 6th IEEE Conference on Nanotechnology, Cincinnati, OH, July 16-20, 2006.
3. Hongguo Zhang and Zhi Chen, "Growth of Horizontally Aligned One-Dimensional Carbon Nanotubes Array on a Si Substrate," the 6th IEEE Conference on NanotechnologyCincinnati, OH, July 16-20, 2006.
4. Dongyan Ding and Zhi Chen, "Detecting high concentration hydrogen with nanoporous palladium supported by anodic aluminum oxides," the 64th Device Research Conference, IEEE, University Park, PA, June 26-28, 2006. pp. 127-128.
5. Z. Chen and K. Saito, "Novel Carbon Nanotube-Based Nanostructures for High-Temperature Gas Sensing," Abstract for US Department of Energy UCR program PI Meetings, Pittsburgh, PA, 06/06-06/08/2006.
6. Z. Chen and K. Saito, "Novel Carbon Nanotube-Based Nanostructures for High-Temperature Gas Sensing," Abstract for US Department of Energy UCR program PI Meetings, Pittsburgh, PA, 06/07-06/09/2007